# Electron-impact ionization of Mg

R. F. Boivin† and S. K. Srivastava
Jet Propulsion Laboratory,
California Institute of Technology,
4800 Oak Grove Drive, Pasadena,
California, USA, 91109-8099

‘NRC-NASA Resident Research Associate

**Abstract.** A pulsed crossed beam technique is used to measure ionization cross-sections of metallic atoms. Relative values of cross-sections of single, double and triple ionization of magnesium have been successfully measured with good accuracy over the **0-700 eV** range. Absolute values of cross-sections have been obtained by normalization to a theoretical value at high electron energy. Results are compared to previously published values and, for single ionization in particular, a comparison with theoretical cross-sections is performed,

## 1. Introduction

Most astrophysical plasmas are in non-LTE (local thermal equilibrium) (see for instance, Shun [1982], Raymond [1977]) and require a vast variety of atomic data for modeling purposes. In particular, ionization rates for various atomic species found in astrophysical plasmas are of great importance. In the past, Lotz classical-imperical formula [1967] has been extensively used to calculate ionization rates. However, recent measurements and improved theoretical calculations are clearly indicating that Lotz rates are not accurate and may be in error by as much as a factor of three. Arnaud and Rothenflug [1985] have improved this situation and generated ionization cross sections for 15 elements. In general there is agreement with previous results. However, for metal atoms the situation is still far from being satisfactory.

Experimental determination of ionization cross sections for metal atoms is not an easy task due to several difficulties. First, most metal atoms require high temperatures to form their vapors. Second, in order to obtain cross sections values, absolute number densities in vapor phase are needed. Therefore, these cross sections have been measured only by very few experimental groups and for a limited number of elements. Magnesium is among that select list. It is an astrophysically important atom since its emission spectra has been recorded by several ground based and spacecraft based instruments Jefferies [1991]. In the seventies, Vainshtein et al. [1972], Okudaira et al. [1970], Okuno et al. [1970] and, Karstensen and Schneider [1975 and 1978] measured the electron impact ionization cross-section for magnesium. More recently Freund et al. [1991] and McCallion et al. [1992] have published cross-section values for Mg. On the theoretical front, Peach [1966, 1969] has calculated ionization cross-section for the Mg atom using a number of theoretical models such as the Coulomb-Born, Born-exchange, Born-Ochkur and modified Coulomb-Born approximations. Mcguire [1977] used the generalized oscillator strength approximation to calculate the single ionization cross-section for magnesium, The emerging picture in terms of cross-section for Mg is getting clearer, however a great spread in cross-section values still exist. The accuracy and validity of the new experimental data is subject to confirmation by other groups which could use different experimental techniques for cross section measurements. Thus, for all the reasons mentioned above, we have chosen magnesium as our first metal atom for ionization cross-section measurement.

## 2. **Experimental approach**

### 2.1 Experimental apparatus

A detailed description of the experimental arrangement has been discussed earlier (Krishnakumar and Srivastava [1988]) and only a brief description of the main features will be presented here. For comprehension purposes, the experimental apparatus can be separated in three components: the electron beam system, the extraction/detection system and the metal beam generator. A simplified version of the experimental apparatus is shown in Fig. 1.

#### 2.1.1 Electron beam system.

A three element pulsed electron gun is used to generate the electron beam. A pulse generator provides pulses of 100 ns duration every 10 μs to the electron gun optics. A Faraday cup is used to monitor the current during the experiment (typically ~ 2 μA). The energy of the electrons is varied from O to 690 V. The current intensity is constant for the entire energy range. The electron beam diameter is less than 1 mm (inferred from the burnt spot on the Faraday cup surface). The electrons go through an open solenoid where they intersects the Mg metal beam at a right angle. The collimating magnetic field inside the solenoid is maintained at 100 mGauss. A gas capillary is also mounted perpendicularly above the electron beam, The capillary extremity is co-axial with the

crucible aperture, thus forming a right angle with the electron beam (the capillary end and the crucible aperture are located within the same plane, the electron beam being at normal incidence). Pressure inside the vacuum chamber is typically kept at about 1 x 10-7 Torr during the Mg emission, Electron beam energy is calibrated by measuring the ionization threshold of Xe which is accurately known (Rosenstock et al. [1977]). A correction of about 1 V is found for filament misalignment and contact potential effects.

2.1.2 Extraction/detection system

Immediately (~100 ns) after every electron pulse, a second pulse generator (triggered by the first) provides an extraction pulse to the extraction grids. The ion extraction field is produced by the application of pulses of 40 V in amplitude and about 1 μs in duration between a pair of extraction grids located on each side of the beam intersection region (see Fig. 1). Optimization of amplitude, duration and delay parameters for the extraction pulses was performed to ensure that the maximum of the newly formed ions were collected. The ions were then collected and focused at the entrance of the mass spectrometer through a series of electrostatic lenses. A channeltron particle detector was used to count each collected ion. The multichannel analyzer accumulated and stored for each channel (1024) the number of count. The extraction/detection system can be used in two distinct modes: single mass detection and mass spectrum detection. In the single mass detection mode, the spectrometer is tuned to a specific mass and the electron energy is varied from O to 690 V. Energy resolution is 0.67 V per channel. The extraction

system is also being used in the mass spectrum mode. In this mode the electron energy is fixed and the mass spectrometer scan to obtain the mass spectrum. Mass resolution is about 0.1 amu per channel.

### 2.1.3 Metal beam source

The metal beam source consisted of a molybdenum crucible filled with a 99.8 % pure magnesium powder (Goodfellow [1997]), The cylinder shape crucible had a small circular aperture ($\Phi$ = 0.123 mm) on top from which the vaporized Mg escaped to form the metal beam. In the intersection region, the diameter of the Mg beam was estimated to be about 4 mm (measured by triangulation from the Mg deposition surface located on the base of the capillary holder). A tungsten filament was placed underneath the crucible. The filament was slowly brought to a potential of about 900 V with respect to ground. A current of a few amperes was circulated through the filament. The thermo-emission of the filament (emission current) was used to heat the crucible and consequently vaporize the magnesium powder. A platinum-rhodium thermocouple was used to measured the temperature of the crucible. Temperature range for magnesium vaporization was observed between 425 and 500 “C (the vaporization temperature being a function of the pressure inside the crucible).

## 2.2 Ionization efficiency curves and normalization.

The ionization efficiency curves showing the variation of the relative ion intensity as a function of the electron impact energy for the various Mg ions were obtained under the following conditions.

1) Stable electron current. The electron gun gave a steady current during all measurements.

2) Constant extraction conditions. All extraction conditions for ions remained the same during all measurements (Mg, Xe and Ne (see section 3.2)).

3) Stable crucible temperature. The crucible temperature remained constant (within ± 10 ‘C ) during each Mg ionization efficiency curve measurement.

4) Mg was the dominant atom in the extraction beam, Mg was the highest peak in the mass spectrum before any Mg ionization efficiency measurement was made.

5) Frequent electron energy calibration. Electron energy calibration was performed after each ionization curve measurement (Xe threshold measurement).

6) Verification of the extraction system. Xe ionization efficiency curve was measured immediately after every measurement of Mg ionization efficiency curve. Shape agreement between Xe curves and previously published cross-section (Krishnakumar and Srivastava [1988]) was within 3%.

7) Statistics. The number of count per channel is such that the error associated with random statistical noise on any given channel is negligible.

By definition, the ionization efficiency curves represent the variation of the ion formation intensity as a function of electron impact energy. In the crossed electron-atomic

beam mode, the ion intensity I(E) is related to the ionization cross-section $\sigma(E)$ by the following expression:

$$I(E) = K(m)\,\sigma(E) \int_{v} p(r)\, f_e(\mathbf{r}, E)\, \Delta\Omega(\mathbf{r})\, dr \qquad (1)$$

where I(E) is the number of ions detected per second as a function of incident electron energy E, K(m) is an ion-mass dependent factor which includes the combined efficiency of transmission of ions through the extraction grids, ion optics and quadruple mass analyzer and the detection efficiency of the charged particle detector. The $\mathbf{p(r)}$, $f_e(\mathbf{r}, E)$ and $\Delta\Omega(\mathbf{r})$ functions are respectively the target density, the spatial electron flux distribution and the solid angle of detection for a collision point located at $\mathbf{r}$ within the intersection volume of the two beams. If we assume that the spatial electron flux distribution is independent of the incident electron energy, and considering the special case of the Mg metal beam, equation (1) can be written as:

$$I_{Mg^+}(E) = K(m_{Mg^+})\; G_{Mg}\; \sigma_{Mg^+}(E) \qquad (2)$$

where $K(m_{Mg^+})$ is the combined transmission-detection factor for the singly charged Mg ion and $G_{Mg}$ is a geometric function related to target density, solid angle of detection and electron spatial distribution. The ion detection intensity is now directly proportional to the

magnesium ionization cross-section. Normalization to an absolute value for the cross-section is possible with a single value of the ionization cross-section.

## 3. **Results and discussion**

### 3.1 Mass spectrum and ionization efficiency curve measurement

The crucible is heated to a temperature where the magnesium is detected by the spectrometer. The spectrometer is set to the mass spectrum mode and a series of the mass spectrum are perform at different electron energies (25, 50, 75, 100, 200, 300, 400, 500 and 600 eV). Of particular interest are the mass spectra obtained at 25,100 and 400 eV shown in the Fig. 2. At 25 eV, apart from the usual vacuum contaminants ($H_2O$, CO and $CO_2$), only the singly ionized Mg is seen in the mass spectrum. This is because of the fact that the electron energy is too low to create double or triple ionized magnesium. The $Mg^+$ secondary peaks (mass 25 and 26) are of course associated to the Mg isotopes which have a 10 and 110/0 natural abundances, respectively (Weast [1983]). At 100 eV, both single and double ionized Mg peaks are clearly visible. Note also that the impurities-$Mg^+$ peak ratios are quite larger than in the previous spectrum. This is due to two factors: first and foremost, that the single ionization cross-section for magnesium is much larger at 25 eV than 100 eV (see section 3.2) and second, that for contaminants, the situation is reverse, $H_20$ and $C0_2$ ionization cross-section maximums have been previously observed at 120 and 110 eV, respectively (Rao et al. [1995], Srivastava and Nguyên [1987]). At 400 eV,

single, double and triple ionized Mg are present in the spectrum. Note also, that at this energy, the $Mg^{2+}$ peak is now of the same order of magnitude than the single ionized Mg peak. This situation translates into comparable ionization cross-section values at 400 eV. This subject will be discussed further in section (3.3).

The spectrometer is set in the single mass detection and the single, double and triple ionization efficiency curves are obtained as a function of energy. The single ionization efficiency curve is then normalized to obtain absolute values for the cross-section. For normalization, we have chosen the cross-section value obtained by McGuire [1977] using the generalized oscillator strength approximation at 500 eV. There are a number of reasons to justify this choice. First, the generalized oscillator strength approximation is believed to be very good to predict the ionization cross-section at high energy (Mcguire [1977]). Second, a different model based on a modified Coulomb-Born approximation (Peach [1969]) yields exactly the same value for the cross-section at this particular energy (see Fig. 3). Third, previous experimental results from two independent groups also converge toward this value of 6.50 x $10^{-17}$ $cm^2$ at 500 eV (see Fig. 4). Finally, let us mention that is this region the decrease of the cross-section as a function of energy is slow and is independent of strong fluctuations associated with the ionization threshold as well as potential effect related to metastable magnesium atoms (Shafranyosh and Margitich [1 996]).

3.2 Single ionization cross-section for magnesium

Our experimental ionization efficiency curve is normalized by using McGuire's [1977] calculated cross-section at 500 eV and shown in Fig. 3. McGuire's [1977] cross-section values, calculated using the generalized oscillator strength approximation is also shown in Fig. 3. The overall agreement between calculations and experiment is quite good. As expected, excellent agreement is found in the 300 to 500 eV range. However, our cross-section value at maximum is 13% lower than the calculated cross-section. Note also, that in the 60 to 250 eV range our cross-section values are about 9°/0 larger than those predicted by McGuire [1977]. Calculated ionization cross-sections for the magnesium atom using a modified Coulomb-Born approximation (Peach [ 1969]) are shown in Fig, 3. This model takes into account inner shell contributions to the ionization cross-section. The general agreement between model and experiment is also very good. In this case, the maximum cross-sections are only 5.4% apart, the calculated value being slightly larger. Excellent agreement (within 5°A or less) is found in both the 40 to 120 eV and 400 to 700 eV ranges. In the 120 to 400 eV region, the calculated values are about 7°A larger than the experimental cross-sections. Note also, that for almost the entire energy range the experimental data are located between the two theoretical cross-section curves.

A fit is performed on our 1024 experimental cross-section measurements, and this fit is shown in Fig.4. From this fit, cross-section values for specific electron impact energies are shown in 1. All previous experiments featuring the measurement of single ionization of Mg are included in Fig 4. The single ionization cross-sections measured by McCallion et al. [1992] for energies up to 5.3 KeV are compared to our experimental

results. Excellent agreement is found on our entire energy range. However, their maximum cross-section value is 7°/0 higher than ours and their cross-sections values in the 450 to 700 eV are about 16% lower than our cross-sections, Cross-sections measured by Freund et al. [1990] for energies up to 200 eV are also in good agreement with our experimental values. Their maximum cross-section is less than 4°/0 higher than ours while their cross-sections in the 100 to 200 eV range are about 10% higher than ours. Note that McCallion [1992] et al. have used Freund et al. [1990] cross-sections in the 20-40 eV range to normalize their ionization efficiency curve. Cross-sections measured by Okudaira et al. [1970] for energies up to 1200 eV are compared to our present results. At low energy (less than 200 eV) a poor agreement is found, their cross-section values being systematically larger by a factor of 1.8 with respect to ours. At high energy (500 and higher), the agreement becomes increasingly better (13% and 7'% difference at 500 and 600 eV, respectively).

The single ionization cross-section measured by Karstensen and Schneider [1978] were performed from threshold to 200 eV. The overall agreement with our data is poor. At peak value their cross-section is 50% higher than ours. Note also, that their cross-section peak is located at 12 eV which is about 7 to 8 eV below the average peak energy measured by different experiments. This suggests an improper energy calibration or that their experiment is plagued with metastable Mg atoms which have a maximum ionization cross-section at 13 eV (Shafranyosh and Margitich [1996]). Only between 30 and 60 eV and for energy near 200 eV does the two cross-section functions show a good match. Between 70 and 160 eV their cross-section curve shows a bump not observed in our

experiment. Although the cross-sections measured by Vainshtein et al. [1972] are really total ionization cross-section, they may be compared to our present results. This is because their measurements were only made for energy up to 200 eV where single ionization is the dominant ionization process. At peak energy, their cross-section is 1 So/O smaller than ours and the general agreement is poor. The only good match is found in the 40 to 60 eV range. At higher energy (70 to 200 eV) the energy dependence of their cross-section is quite different than what has been observed by our group and by everyone else. Here again, the cross-section peak is observed at 25 eV which indicate a poor energy calibration.

For comparison purposes, all peak cross-section values (experimental and theoretical) and associated electron energy are shown in Table 2. It is now apparent that the maximum value for single ionization cross-section is between 5.0 and 5.5 x $10^{-16}$ $cm^2$, and that this peak is located at about 20 eV. It is also clear, by looking at Figs 3 and 4 that, apart from absolute values at low energy, both the generalized oscillator strength approximation (McGuire [1977]) and the modified Coulomb-Born (Peach [1969]) are adequate to described the energy dependence of the Mg ionization cross-section.

3.3 Double ionization cross-section,

Under the same condition as described in the previous section, the double ionization intensity $I_{Mg^{2+}}(E)$ is related to the double ionization cross-section $\sigma_{Mg^{2+}}(E)$ by the following expression:

$$I_{Mg2+}(E) = K(m_{Mg2+})\ G_{Mg}\ \sigma_{Mg2+}(E) \qquad (3)$$

where $K(m_{Mg2+})$ is the combine transmission-detection factor for the doubly charged Mg ion. By dividing equation (3) by equation (2) and simplifying we obtain:

$$\sigma_{Mg2+}(E) = \frac{I_{Mg2+}(E)}{I_{Mg+}(E)} \frac{K(m_{Mg+})}{K(m_{Mg2+})} \sigma_{Mg+}(E) \qquad (4)$$

where the double ionization cross-section is now expressed in terms of the single ionization cross-section and of two ratios: Intensity and combine transmission-detection ratios. The first ratio can be measured directly from the mass spectrum (see section 3.1), the second ratio, however, represents a more challenging problem. As is the case for all spectrometers, sensitivity often depends on mass to charge ratio. To evaluate the K ratio, we used a gas with similar fragment patterns and with well known single and double ionization cross-sections. In the past, our group has performed a complete study of rare gas atoms by electron impact (Krishnakumar and Srivastava [1 988]). In this case, Ne with observable fragments at 19.992, 9,996 and 6,664 amu (which closely compare to 23.985 11,993 and 7,995 amu for Mg), is used to evaluate the K ratio. Rewriting equation (4) in terms of the neon K ratio, we have:

$$\sigma_{Mg2+}(E) \approx \frac{I_{Mg2+}(E)}{I_{Mg+}(E)} \frac{K(m_{Ne+})}{K(m_{Ne2+})} \sigma_{Mg+}(E) \qquad (5)$$

Intensity ratios are measured for Neat different energies (100, 200, 300,400, 500 and 600 eV) in the mass spectrum mode and used with the previously publish cross-sections (Krishnakumar and Srivastava [1988]) to evaluate the K ratio. Combining the K ratio values with Mg ion intensity ratios measured in the mass spectrum mode (section (3. l)), a normalization factor is obtained. This factor is then multiplied by the single ionization cross-section at a specific energy, thus providing the absolute normalization factor for the double ionization efficiency curve. The resulting cross-section for double ionization is shown in Fig. 5. A fit has been performed on our experimental data and specific cross-section values are shown in 1. The results of previous experiments are also shown in Fig. 5. Of particular interest, the 40 to 60 eV region, where a discontinuity in the cross-section function can be seen. This discontinuity has been observed by both McCallion et al. [1992] and by Okudaira et al. [1970] and has been interpreted to be due to the following Auger transition (Peach [1970]):

$$Mg^{+}\,(2p^{5}3s^{2}\ 2P) \Longrightarrow Mg^{2+}\,(2p^{6}\ {}^{1}S) + e^{-} \qquad (6)$$

where this auto-ionization takes place immediately after removal of a 2p electron at 55.8 eV (Fiquet Fayard et al. [1968] and Slater [1955]). Thus, two distinct processes are believed to contribute to the total double ionization cross-sections: direct double ionization (which start at 22.68 eV Moore [1971]) and Auger transition (which start at 55.8 eV). As indicated by the smooth curve in Fig. 5, and confirmed by earlier measurements (Fiquet Fayard et al. [1968]) the double ionization process is, for energies

higher than 60 eV, dominated by Auger transitions. The fact that Auger double ionization is really a simple ionization (of a inner shell electron) followed by an auto-ionization also explains why the double ionization cross-section is unusually high compare to the single ionization cross-section. Double ionization cross-sections measured by McCallion et al. [1992] are compared to the present values. A good agreement is found for electron energies higher than 100 eV. Note that their data exhibit a greater scatter than our measured cross-sections. At low energy (20 to 40 eV), our cross-sections are however about 40% larger than the values obtained by McCallion et al. [1992]. The double ionization cross-sections obtained by Okudaira et al. [1970] are in reasonable agreement with our present values. At low energies, the agreement is good (within 10%) with both measurements showing the same Auger structure. At high energies, their cross-section is about 33°/0 larger than ours. Finally, cross-sections measured by Karstensen and Schneider [1978] are considerably different than ours in both magnitude and energy dependence. The overall agreement with our data is very poor. Problems with calibration technique or/and measuring procedure are suspected for this disagreement.

3.4 Triple ionization cross-section

In a similar fashion, the triple ionization cross-section for magnesium are measured and normalized. In this case, we used, as described in the previous section, the K ratio for simple and triple ionized Ne atom to normalize the triple ionization efficiency curve

obtained for Mg. Using equation (5), and rewriting it in terms of the triple ionization cross-section we have:

$$\sigma_{Mg^{3+}}(E) \approx \frac{I_{Mg^{3+}}(E)}{I_{Mg^{+}}(E)} \frac{K(m_{Ne^{+}})}{K(m_{Ne^{3+}})} \sigma_{Mg^{+}}(E) \qquad (7)$$

The resulting cross-section for triple ionization is shown in Fig. 6. A fit has been performed on our experimental data and specific cross-section values are shown in Table 1. The results of previous experiments are also included in Fig. 6. The triple ionization cross-sections measured by McCallion et al. [1992] are compared to our experimental values. The overall agreement is good. On average their cross-sections are about 15°/0 smaller than ours. Their data also exhibit a larger scatter than ours and fail to locate the threshold (102.8 eV, Moore [1971]) for the triple ionization process. The cross-sections measured by Okudaira et al. [1970] are in good agreement with present results. The ionization efficiency function is almost identical and their absolute cross-section values being on average only 7% higher than ours.

3.5 Discussion of errors

The uncertainties associated with single, double and triple ionization cross-sections are essentially composed of two independent sources: error related to the shape of the ionization efficiency curves and the error in the calibration factors used to normalize the curves. In all cases, the uncertainties related to the shapes of ionization efficiency curves

is much smaller than the errors associated with the normalization. Thus, for all cross-section curves, the error is essentially systematic and related to the absolute normalization factor.

For single ionization, the principal source of error is the calibration factor used to normalize the ionization efficiency curve. In this case we used the Mcguire [1977] calculations at 500 eV to normalize our curve. As mentioned earlier (see section 3.1) this model is believed to be very good to predict cross-section a high electron energy. We assumed a ± 10OA error for this normalization factor and a ± 3°A error for the shape of the ionization efficiency curve (see section 2.2). This translates into a ± 11°/0 error bar for the single ionization cross-section. For double ionization, the resulting uncertainty must also include errors associated with the Ne single and double ionization used to evaluate the K ratio (see section 3.3). These errors have been evaluated previously (Krishnakumar and Srivastava [1988]) and are* 10% and ±13%, respectively. The resulting uncertainty for double ionization is, therefore, estimated to be ±19%. Similarly, for triple ionization, errors associated with Ne single and triple ionization cross-section (± 10°/0 and ± 22°/0, respectively) are included and, the resulting uncertainty is estimated to be ± 25°/0.

## 4. **Conclusion**

Cross-sections for single, double and triple ionization of magnesium by electron impact have been measured in the O to 690 V range. For single ionization, a good agreement between present results and calculated cross-sections using either the

generalized oscillator strength approximation or the modified Coulomb-Born approximation is found. The present results are also in good agreement with the latest published cross-sections. For double and triple ionization cross-sections, reasonable agreements between present measurements and previously published cross-sections are found.

**Acknowledgments**

The research reported in this paper was carried out at the Jet Propulsion Laboratory and was sponsored by the National Aeronautics and Space Administration. One of us (RFB) would like to thank NRC, Washington, DC, for a Resident Research Associateship grant during the course of this work.

## References


Arnaud M and Rothenflug R 1985 Astrophys. Suppl, Ser. 60425

Weast R C Ed. 1983 CRC Handbook of Chemistry and Physics, Table of Isotopes B-258

DrinkWine M J and Lichtman D 1980 Partial Pressure Analysers and Analysis, Monograph Series, edited by Whetton N R and Lang R, American Vacuum Society, New York

Fiquet-Fayard F, Chiari J, Muller F and Ziesel J P 1968 J Chem. Phys.48 1478

Freund R S, Wetzel R C, Shul R J and Hayes T R 1990 Phys. Rev. A **413575**

Goodfellow [1997] Technical Data Sheet

Jefferies J T1991 Astrophys. J. 377,337

Karstensen F and Schneider M 1975 Z.PhysA273321

Karstensen F and Schneider M 1978 J. Phys. B: At. Mol. Phys. **11167**

Krishnakumar E and Srivastava S K 1988 J. Phys. B: At Mol. Opt. Phys. 211055

Lotz W 1968 Z. Phys. 216241

McCallion P, Shah M B and Gilbody 1992 J Phys. B: At Mol. Opt. Phys. 251051

McGuire E J 1977 Phys. Rev. A **1662**

Moore C E 1971 Atomic Energy Levels, Vol 1, Natl. Bur. Stds., NSRDS-NBS 35

Okudaira S, Kaneko Y and Kanomata I 1970 J. Phys Sot. Japan 281536

Okuno Y, Okuno K, Kaneko Y and Kanomata I 1970 J. Phys. Sot. Japan 29164

Peach G 1966 Proc. Phys. Sot. 87375

Peach G 1970 J. Phys. B: At. Mol. Phys. 3328

Rao M V V S, Iga I and Srivastava S K 1995 J. Geophys. Res. **100421**

Rosenstock H M, Draxl K, Steiner B W and Herron J T [1977] J. Phys. Chem. Ref. Data, 6, Suppl. 1

Raymond J R and Smith B W 1977, Astrophys. J. Suppl. 35,419

Shafranyosh I I and Margitich M O 1996 Z. Phys. D 3797

Shun J M 1982, Astrophys. J. 262,308

Slater J C 1955 Phys. Rev. 981039

Srivastava S K and Nguyên H P 1987 NASA/JPL Publication No 87-2

Vainshtein L A, Ochkur V I, Rakhovskii V I and Stepanov A M 1972 Sov. Phys.-JETP 34 271

Table 1. Cross-sections for single, double and triple ionization of magnesium by electron impact.

Table 2. Comparison of cross-section peak values for single ionization.

Fig. 1. Schematic diagram of the experimental apparatus. 1- High voltage P. S., 2- High current P. S., 3- Tungsten filament, 4- Emission current meter, 5- Thermocouple, 6- Crucible, 7- Metallic powder, 8- Metal beam, 9- Electron beam, 10- Extraction grids, 11- Gas capillary, 12- Enzel lenses, 13- Quadruple mass analyzer, 14- Detector, 15- Amplifier, 16- Multichannel analyzer.

Fig. 2. Mass spectrums featuring Mg ions observed at different electron energies (25, 100,400 eV).

Fig.3. Single ionization cross-section of Mg by electron impact. Theory: (———) Mcguire [1977]; (---------) Peach [1969]; (·····) Present results.

Fig. 4. Single ionization cross-section of Mg by electron impact. (—--) Present data; (00000) Karstensen and Schneider [ 1978]; (□□□□□) McCallion et al. [ 1992]; (ΔΔΔΔΔ) Freund et al. [1990]; (∇∇∇∇∇) Vainshtein et al. [1972]; (■ ■ ● ■ ■ ) Okudaira et al. [1970].

Fig. 5. Double ionization cross-section of Mg by electron impact. (———-) Present data; (00000) Karstensen and Schneider [1978]; (□□□□□) McCallion et al. [1992]; (m¤¤¤¤ ) Okudaira et al. [1970].

Fig. 6. Triple ionization cross-section of Mg by electron impact. (———-–) Present data; (□□□□□) McCallion et al. [1992]; (■ ■ ■ ■ ■ ) Okudaira et al. [1970].

Table 1 Cross-sections for simple, double and triple ionization of magnesium by electron impact

| Electron Energy (eV) | $\sigma_1$ ($10^{-16}$ cm$^2$) | $\sigma_2$ ($10^{-17}$ cm$^2$) | $\sigma_3$ ($10^{-18}$ cm$^2$) |
|---|---|---|---|
| 5.0 | 0.000 | | |
| 10.0 | 2.100 | | |
| 15.0 | 4.566 | | |
| 20.0 | 5.080 | 0.000 | |
| 25.0 | 4.926 | 0.049 | |
| 30.0 | 4.731 | 0.124 | |
| 35.0 | 4.499 | 0.236 | |
| 40.0 | 4.232 | 0.324 | |
| 45.0 | 3.972 | 0.364 | |
| 50.0 | 3.733 | 0.385 | |
| 55.0 | 3.513 | 0.436 | |
| 60.0 | 3.312 | 0.538 | |
| 65.0 | 3.128 | 0.643 | |
| 70.0 | 2.959 | 0.745 | |
| 75.0 | 2.804 | 0.846 | |
| 80.0 | 2.663 | 0.944 | |
| 85.0 | 2.534 | 1.039 | |
| 90.0 | 2.416 | 1.131 | |
| 95.0 | 2.308 | 1,220 | |
| 100.0 | 2.209 | 1.306 | 0.000 |
| 110.0 | 2.037 | 1.467 | 0.011 |
| 120.0 | 1.893 | 1.614 | 0.030 |
| 130.0 | 1.771 | 1.747 | 0,057 |
| 140.0 | 1.669 | 1.865 | 0.089 |
| 150.0 | 1.582 | 1.969 | 0.126 |
| 160.0 | 1.507 | 2.059 | 0.169 |
| 170.0 | 1.441 | 2.136 | 0.216 |
| 180.0 | 1.383 | 2.202 | 0.267 |
| 190.0 | 1.330 | 2.256 | 0.321 |
| 200.0 | 1.282 | 2.301 | 0.376 |
| 225.0 | 1.175 | 2.374 | 0.519 |
| 250.0 | 1.080 | 2.406 | 0.657 |
| 275.0 | 0.994 | 2.411 | 0.781 |
| 300.0 | 0.916 | 2.400 | 0.885 |
| 325.0 | 0.848 | 2.382 | 0.966 |
| 350.0 | 0.792 | 2.360 | 1.022 |
| 375.0 | 0.748 | 2.337 | 1.055 |
| 400.0 | 0.716 | 2.313 | 1.070 |
| 425.0 | 0.693 | 2.286 | 1.071 |
| 450.0 | 0.677 | 2.255 | 1.064 |
| 475.0 | 0.664 | 2.219 | 1.052 |
| 500.0 | 0.650 | 2.178 | 1.038 |
| 525.0 | 0.633 | 2.132 | 1.023 |
| 550.0 | 0.612 | 2.085 | 1.008 |
| 575.0 | 0.587 | 2.039 | 0.990 |
| 600.0 | 0.560 | 1.997 | 0.967 |
| 625.0 | 0.535 | 1.959 | 0.937 |
| 650.0 | 0.518 | 1.919 | 0.904 |
| 675.0 | 0.513 | 1.862 | 0.877 |

Table 2 Comparison of cross-section peak values for single ionization

| References | Peak cross section values (10-" cm') | Energy at peak value (eV) |
|---|---|---|
| Experimental | | |
| Present experiment | 5.11 | 20.1 |
| Shafranyosh andMargitich[1996] | 5.0* | 20.0* |
| McCallion et al. [1992] | 5.47 | 17.4 |
| Freund et al. [1990] | 5.30 | 20.0 |
| Karstensen and Schneider [1978] | 7.70 | 12.0 |
| Vainshtein et al. [1972] | 4.35 | 25.0 |
| Okudaira et al. [1970] | 9.40 | 18.0 |
| Theory | | |
| McGuire [1977] | 5.85 | 17.0 |
| Modified Born, Peach [1970] | 5.40 | 21.0 |
| Born-Ochkur, Peach [ 1970] | 4.6 | 20.0 |
| Born-Exchange, Peach [1966] | 5.8 | 20.0 |
| Coulomb-Born, Peach [1966] | 6.9 | 20.0 |

*The ionization cross-section has only been measured in the O to 21 eV range.

FIG 1

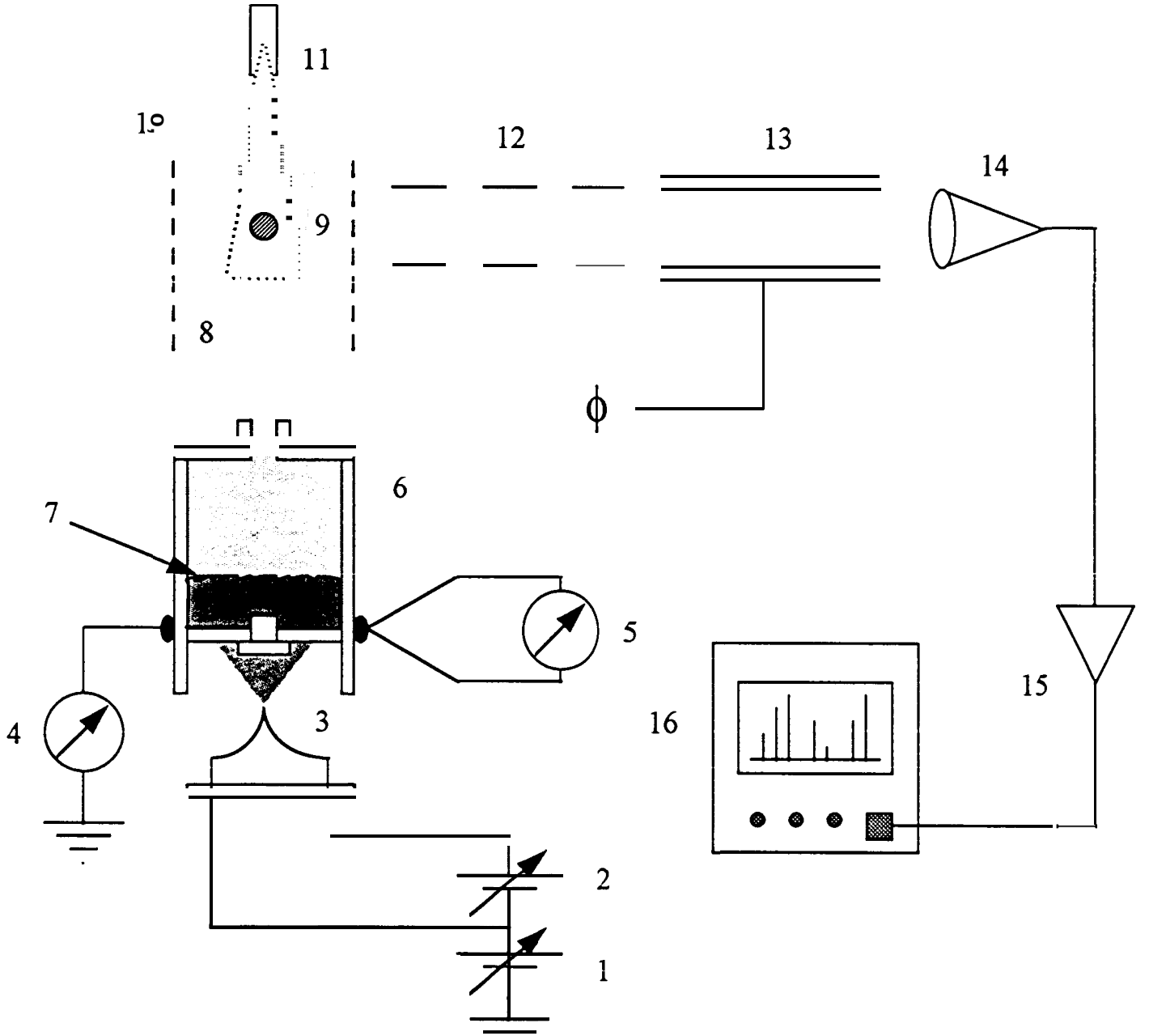

FIG 2

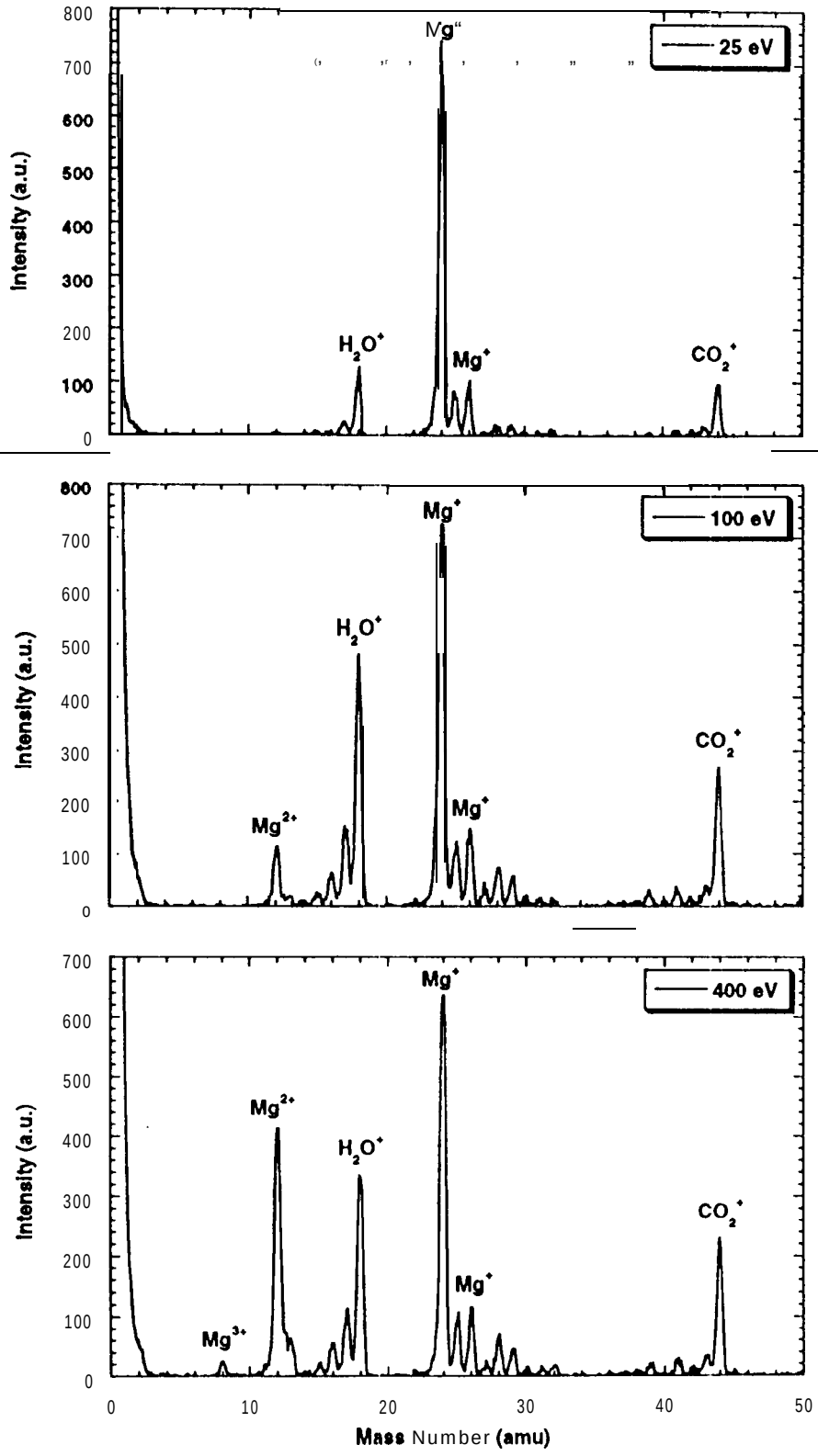
25 eV
100 eV
400 eV
Intensity (a.u.)
Mass Number (amu)
Mg+
H2O+
CO2+
Mg2+
Mg3+

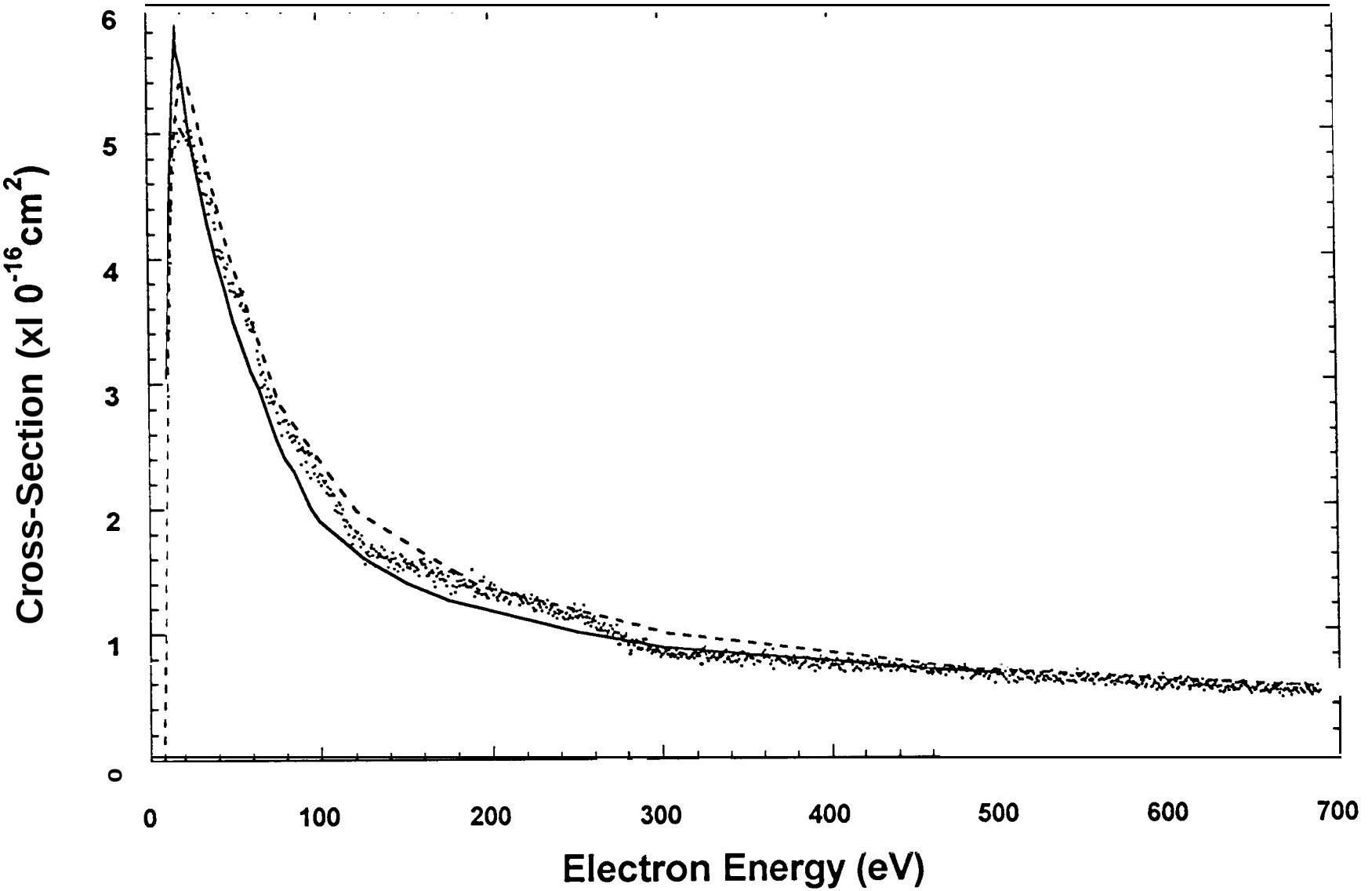
Cross-Section (xl 0^-16 cm^2)
6
5
4
3
2
1
0
0
100
200
300
400
500
600
700
Electron Energy (eV)

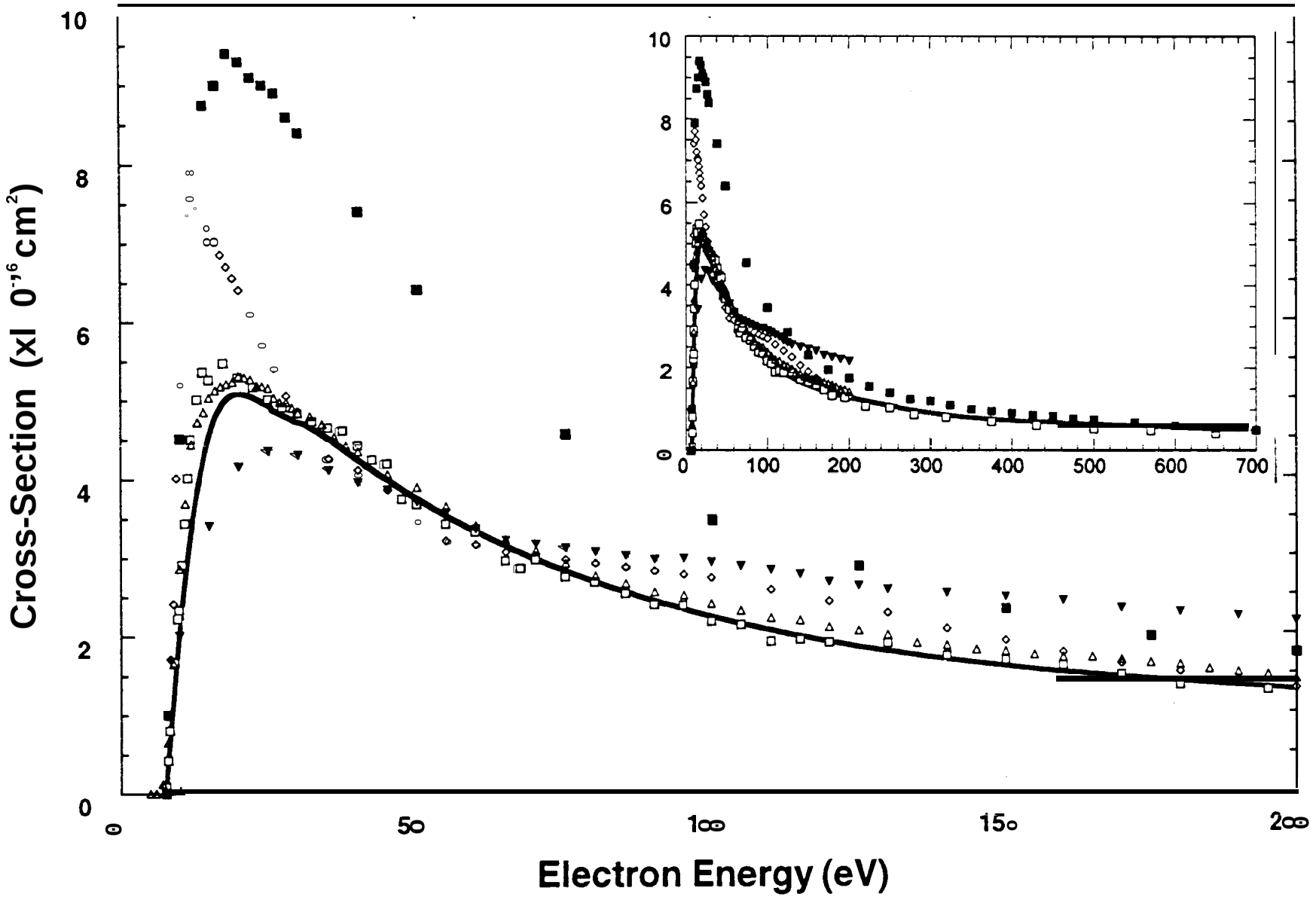
Cross-Section (xl 0⁻¹⁶cm²)
Electron Energy (eV)
0
2
4
6
8
10
0
50
100
150
200
0
2
4
6
8
10
0
100
200
300
400
500
600
700

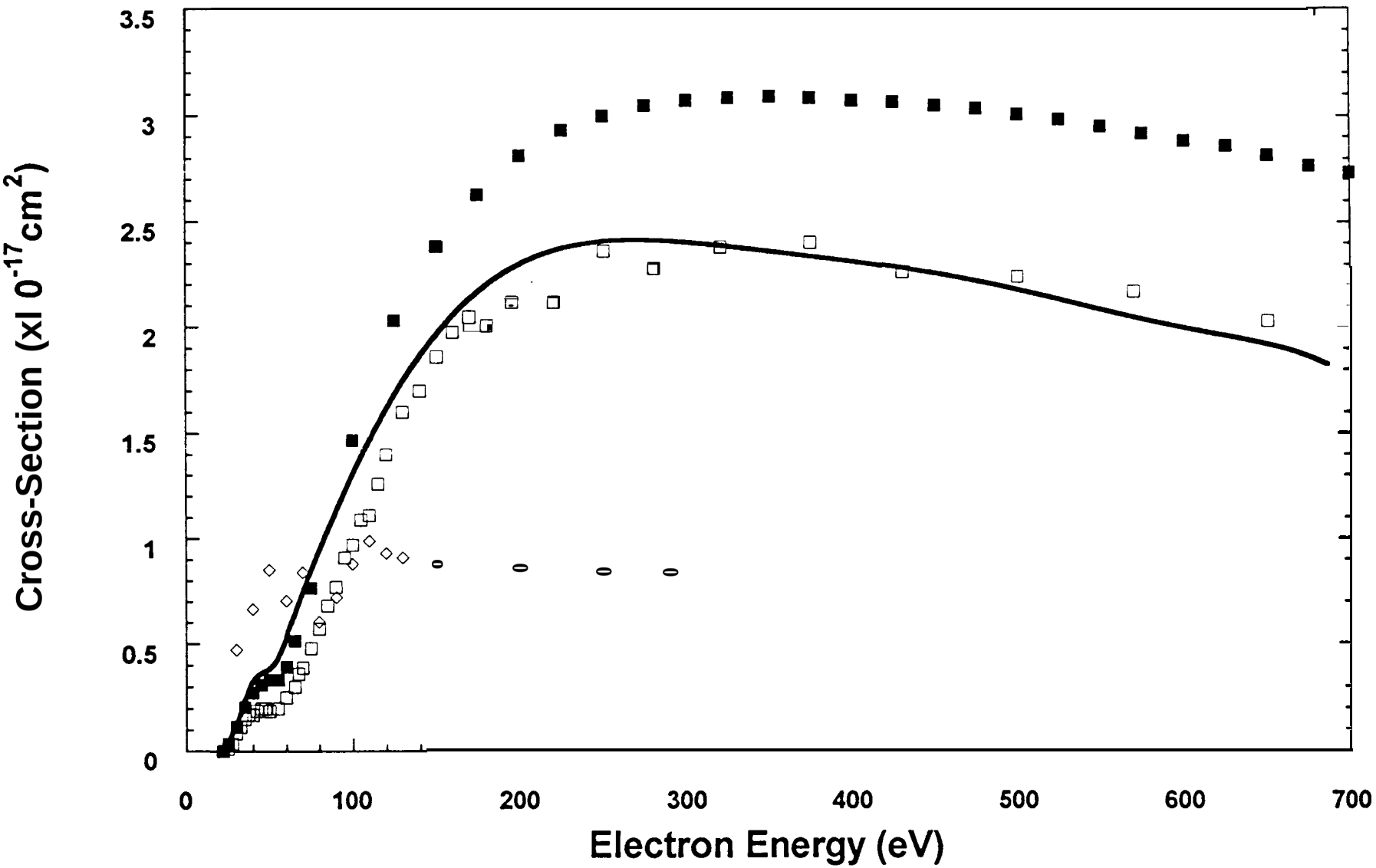
Cross-Section (xl 0$^{-17}$cm$^2$)
3.5
3
2.5
2
1.5
1
0.5
0
0
100
200
300
400
500
600
700
Electron Energy (eV)

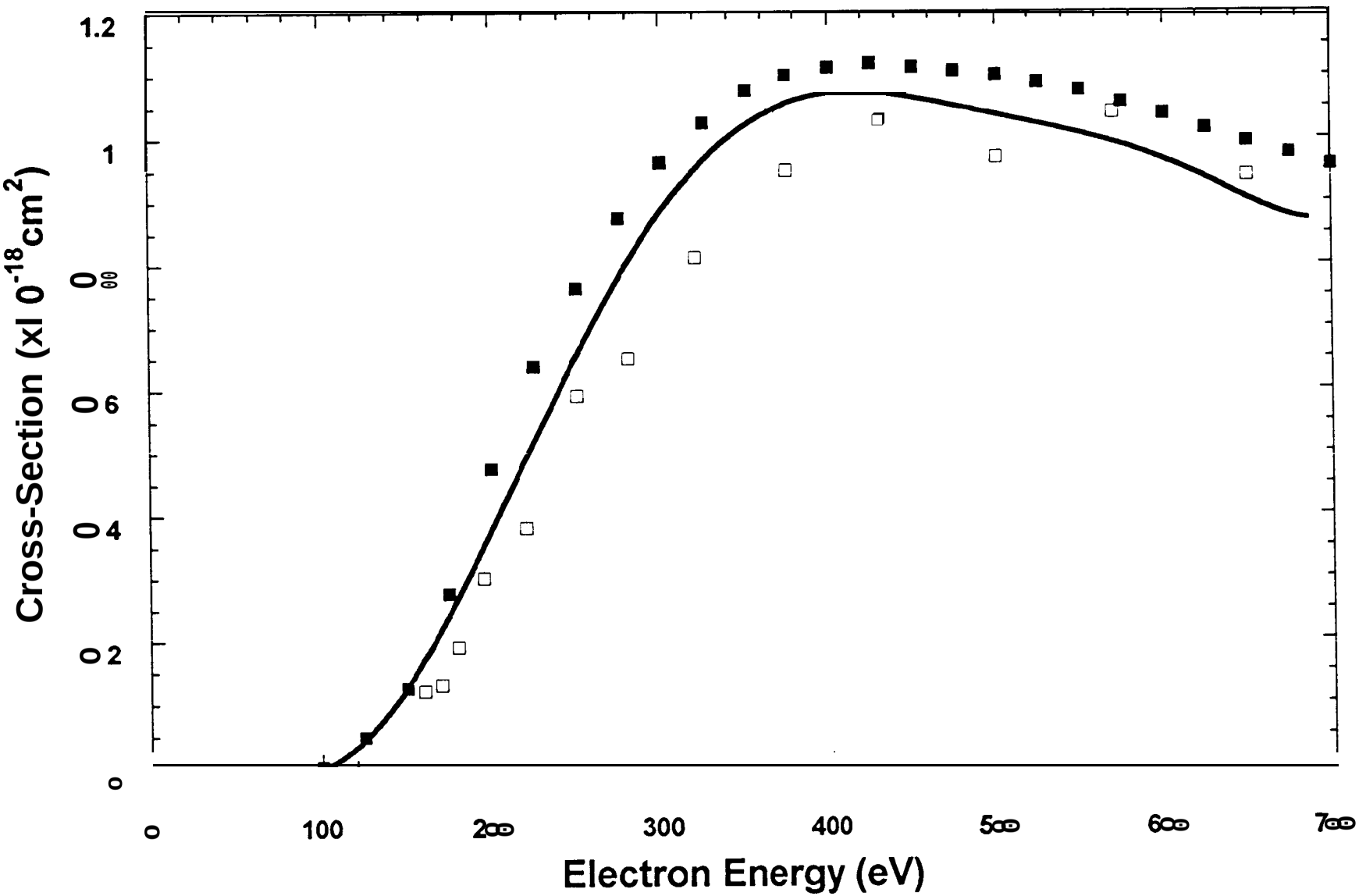
Cross-Section (xl 0-18cm2)
1.2
1
0 6
0 4
0 2
0
0
100
300
400
Electron Energy (eV)